Arab J Geosci (2016) 9: 313
DOI 10.1007/s12517-016-2338-5

ORIGINAL PAPER

Source mechanism and parameters of the 19 October 2012 earthquake, northern Egyptian continental margin

Awad Hassoup[1] · **Mostafa Toni**[2] · **M. M. F. Shokry**[3] · **A. M. A. Helal**[3] · **Emad K. Mohamed**[1]

Received: 9 April 2015 / Accepted: 20 January 2016 / Published online: 5 April 2016

Abstract The 19 October 2012 earthquake (M_L = 5.1) occurred in the northern continental margin of Egypt within the Nile Cone at latitude 32.35° N and longitude 31.27° E. The quake was felt over a wide area in north Egypt and East Mediterranean countries, but no casualties have been reported. This area had experienced the large earthquake (Ms = 6.7) of 12 September 1955. The fault plane solution of the 19 October 2012 earthquake is here presented based on the digital seismograms recorded by the Egyptian National Seismological Network (ENSN) and other regional seismic stations. The analysis is carried out using the well-known techniques of first motion polarities of P-wave and the amplitude ratios of P-, SH-, and SV-waves with lower hemisphere projection. The fault plane solution based on the first P-wave onset demonstrates a left lateral strike-slip faulting mechanism, while the solution based on both P-wave polarities and amplitude ratios of P-, SH-, and SV-waves reveals a reverse fault with strike-slip component trending NW–SE to NE–SW, in conformity with the N–S compression along the Hellenic Arc convergence zone. Following the Brune's model, the source dynamic parameters for the 19 October 2012 earthquake are estimated as corner frequency = 1.47 Hz, fault radius = 0.7 km, stress drop = 22.1 MPa, seismic moment = 2.80E + 16 Nm, and moment magnitude M_w = 4.9. These parameters may provide important quantitative information for the seismic hazard assessment studies.

Keywords Egyptian continental margin · Focal mechanism · Source parameters

✉ Mostafa Toni
mostafa.toni@hq.helwan.edu.eg

[1] National Research Institute of Astronomy and Geophysics (NRIAG), Helwan, Cairo, Egypt

[2] Geology Department, Faculty of Science, Helwan University, Cairo, Egypt

[3] Geophysics Department, Faculty of Science, Ain Shams University, Cairo, Egypt

Introduction

The northern Egyptian continental margin is located to the south of the Mediterranean Sea Ridge where the sea floor is occupied by the Nile Deep Sea Fan, Eratosthenes Seamount, and Herodotus basin. It represents the northeastern portion of the North African passive continental margin (Fig. 1). This region is of great importance due to the hydrocarbon exploration activity there (Badawy et al. 2015).

The northern Egyptian continental margin is characterized by a complex tectonic setting accompanied by earthquake activity due to the relative movement between African and Eurasian plates (Badawy et al. 2015). The structural pattern of this region and its surroundings is shown in Fig. 1. Numerous geodynamic models have been developed to explain the processes in this region (Makris 1976; Le Pichon et al. 1982; McKenzie 1970, 1972; Badawy 1996; Badawy and Horváth 1999a, 1999b; Mascle et al. 2006). One of these models adopted the idea that the northern Egyptian continental margin represents the transition zone between the continental–oceanic crusts where the stress field changes from dominated tension on Egypt land to compression along the Hellenic Arc convergence zone. The Hellenic Arc is a tectonic feature related to the subduction of the African plate beneath the Aegean Sea plate (Sofratom Group 1984; Abu Elenean 1997; Korrat et al. 2005; Abou Elenin and Hussein 2007; Abu El-Nader et al. 2013).

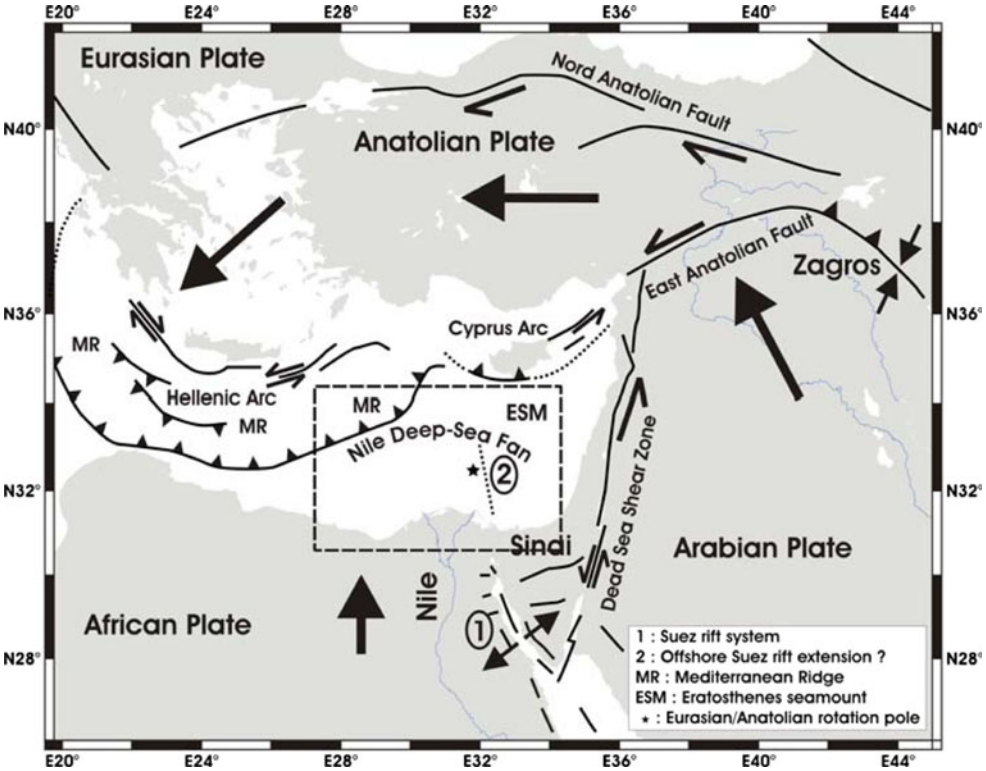

Fig. 1 Tectonic framework of the Eastern Mediterranean region. *Dotted rectangle* shows the area around the epicenter of 19 October 2012 earthquake. *Grey arrows* indicate relative plate motions (after Mascle et al. 2006)

The northern Egyptian continental margin has suffered from historical and instrumental earthquake activity (Maamoun et al. 1984; Ambraseys et al. 1994). Two historical earthquakes with maximum intensity (MSK = VI) were reported on 320 and 956 A.D. and caused considerable damage in north Egypt especially in Alexandria City (Maamoun et al. 1984; Ambraseys et al. 1994; Badawy 1999; Badawy et al. 2015). The earthquake catalogue of Egypt (1900–2014) collected from the Egyptian National Seismological Network (ENSN), National Earthquake Information Center (NEIC), and International Seismological Centre (ISC) demonstrates that the most significant earthquake to have occurred in the Egyptian continental margin was in 12 September 1955 with magnitude Ms = 6.7 (Fig. 2). This event caused notable damage in several localities in the Nile Delta and Alexandria (Badawy et al. 2015). The focal mechanism of this event is a strike-slip faulting mechanism with a considerable reverse component (Costantinescu et al. 1966).

Seismicity of the Eastern Mediterranean region developed by Abou Elenin and Hussein (2007) reveals that almost of earthquake activities tend to be clustered at three zones; the Mediterranean Ridge, Nile Cone, and the Eratosthenes Seamount (Badawy et al. 2015). Korrat et al. (2005) reported that although this region appears to be characterized by a sparse activity, there is a marked concentration of seismic activity in the Nile Cone before and after the installation of ENSN.

In this article, we introduce a detailed fault plane solution for the (M_L = 5.1) 19 October 2012 northern Egyptian continental margin earthquake (Fig. 2). Our estimations based on the first motion polarities of P-waves as well as the amplitude ratios of P-, SH-, and SV-waves. In order to obtain further information about the physical properties of the earthquake source, we also estimate the source parameters of the investigated event including the fault radius, corner frequency, stress drop, seismic moment, and moment magnitude.

Geological and tectonic setting

The passive continental margin of Egypt appears in the south to the folded arc forming the Mediterranean Ridge, where the sea floor is occupied by the Nile Deep Sea Fan, Levant Basin, Eratosthenes, Seamount, and Herodotus basin. Its eastern border is characterized by a narrow continental shelf extending from the shoreline seaward to the shelf edge at about 15–20 km. However, the shelf in the region between Rosetta mouth and Bardawel Lake becomes wider, where it ranges in excess of 70 km (Ross and Uchupi 1977). The Mediterranean Ridge, Levant Basin, and Nile Deep Sea Fan are the major morphostructral domains in the study region. The Mediterranean Ridge is a long accretionary prism between Africa and southern Europe, consisting of sediments which are scrapped off from the subducting plate (McKenzie 1970). Its initial rifting has been dated between Jurassic to Early Cretaceous times (Morelli 1978; Guiraud and Bosworth 1999; Dolson et al. 2000). It is re-activated during

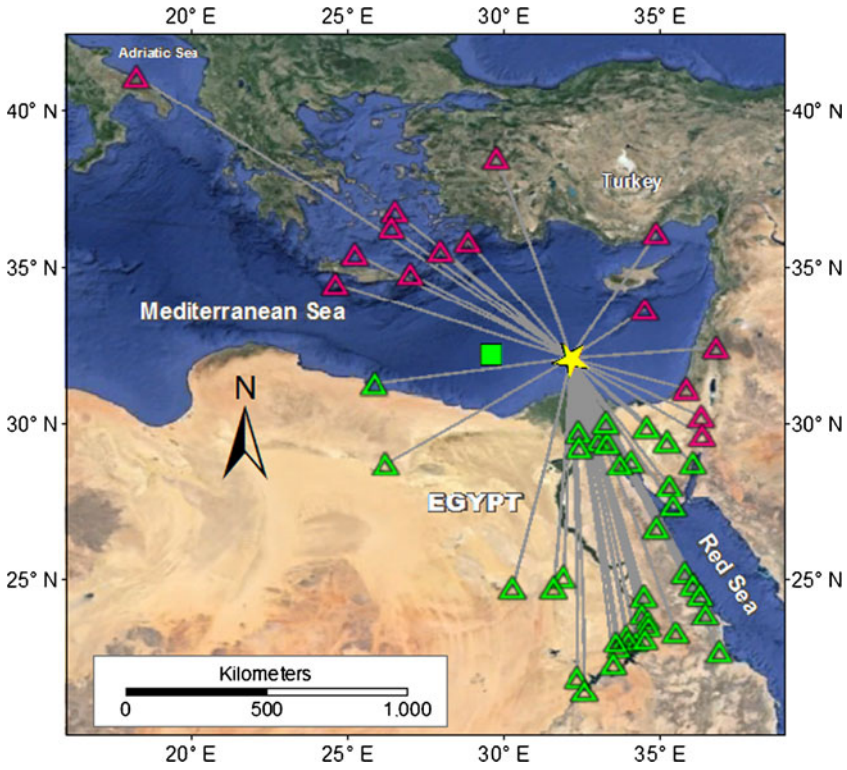

Fig. 2 Location map showing the epicenter of the 19 October 2012 earthquake (*star*) and seismic stations that recorded this earthquake and used in fault plane solution; ENSN stations (*green triangles*), regional seismographs (*red triangles*). The *green square* indicates the epicenter of the 12 September 1955 earthquake

the middle to upper Miocene during the Red Sea–Gulf of Suez rifting (Mascle et al. 2000). Eastward, it is bounded by the Dead Sea Fault zone (DSF), and to the north, by the Cyprus convergent zone and Mediterranean Ridge (MR). The Nile Delta Fan is considered as a large hinge zone that consists of several half grabens to southward. These grabens are deformed and bounded by E-W oriented northward dipping faults (Hussein et al. 2001). The Nile Delta Fan is rich of sedimentary clastic accumulation within the southern Eastern Mediterranean Sea (Ross and Uchupi 1977). This con drapes most of the Egyptian continental margin and consists of thick (up to 3 km) rapidly sedimentation of Pliocene to Quaternary sedimentary blanket emplaced on layers of evaporates or lateral equivalents (Loncke 2002). The thickness of these sediments varies between 1 and 3 km (Camera et al. 2004).

The northern Egyptian continental margin forms the remnant of the Mesozoic Neo–Tethys Ocean with rifting stages in Triassic and characterized by nine identified geomorphological land types: beach and coastal flat, coastal dunes, agricultural deltaic land, sabkhas, fish farms, Manzala lagoon, saltpans, marshes, and urban centers (Robertson 1998; Garfunkel 1998, 2004; EL-Banna and Frihy 2009). Abdel Aal and Lelek (1994) reported six major structural trends delineating the present Nile Delta and the northern continental margin of Egypt (i.e., the E–W Neogene hinge line, NE–SW Rosetta fault trend, NW–SE Temsah structural trend, Pelusium shear zone, NW–SE Red Sea–Gulf of Suez fault trend, and the minor N–S Baltim fault trend). The north Egypt has underwent three subsequent tectonic phases from early Mesozoic to present. The present day stress regime affecting this margin is a compressional stress oriented from N to 30° NW (Abdel Aal and Lelek 1994).

Seismicity

The seismicity of the northern Egyptian continental margin during the period (1900–1997) was taken from different sources such as the International Seismological Centre (ISC) and the National Earthquake Information Center (NEIC) and shows low earthquake activity in this region due to lack of seismic stations in north Egypt. The installation of Egyptian National Seismological Network (ENSN) in 1997 has a great contribution in monitoring the seismic activity in the northern Egyptian margin. After the installation of the ENSN, the annual activity rate increased to 54 events per year with total recorded 864 events within 16 years period (Badawy et al. 2015). Recent studies (e.g., Korrat et al. 2005; Abou Elenin and Hussein 2007; Abu El-Nader et al. 2013; Badawy et al. 2015) indicate that the northern Egyptian continental margin is characterized by moderate and continuous seismic activities. These activities are concentrated in the Nile Cone at the southeastern part of the Mediterranean Sea.

The largest historical earthquakes in the Egyptian continental margin were reported on 320 and 956 A.D. with maximum

intensity MSK = VI (Maamoun et al. 1984; Ambraseys et al. 1994; Badawy 1999; Badawy et al. 2015). The largest notable damage in this region was reported from the 12 September 1955 earthquake. This earthquake took place offshore Alexandria within the Nile Cone, with surface wave magnitude (Ms = 6.7). The 12 September 1955 earthquake struck a quite large area bounded by the entire east Mediterranean basin, including Palestine, Cyprus, and Dodecanese Islands. It was felt over a very wide area in Egypt and caused notable damage in the Nile Delta and Alexandria. The fault plane solution of this event was determined as a reverse faulting with strike-slip component on NW/ENE trending planes (Fig. 3). The horizontal motion on the NW plane is right lateral, while on the ENE plane is a left lateral (Maamoun et al. 1984; Abu Elenean 1993; Ambraseys et al. 1994). Costantinescu et al. (1966) pointed out that on 30 January 1951, an earthquake (Ms = 5.7) was recorded at the periphery of the Nile Cone and continental slope with focal mechanism of dominant normal dip slip faulting associated with minor strike-slip component. Another event with magnitude (M_b = 4.6) took place on 9 April 1987 with epicenter located 100 km west of the 12 September 1955 earthquake. The source mechanism of this event corresponds to a normal fault with a strike-slip component. The two nodal planes trend in SSE and NW directions (Abu Elenean 1993; Korrat et al. 2005).

A nearly similar size event (M_b = 4.7) was recorded on 9 June 1988 at the eastern border of the Mediterranean Ridge. Its focal mechanism demonstrates reverse fault with a strike-slip component on the EW–NW nodal plane. Korrat et al. (2005) mentioned that the best studied event was recorded by the ENSN in 28 May 1998 (M_b = 5.5) with epicenter location at about 200 km northwest of Alexandria in the Nile Cone close to the continual shelf periphery. Its fault plane solution shows reverse fault (Hussein et al. 2001). Figure 3 summarizes the focal mechanisms of the significant earthquakes that took place in the northern Egyptian continental margin. It is clear that most of the fault plane solutions in Fig. 3 are reverse faults showing that the Egyptian continental margin is affected by dominant compressional stress field due to the relative movement between African and Eurasian plates.

Fault plane solution

The digital seismograms of the 19 October 2012 earthquake were collected from the Egyptian National Seismological Network (ENSN) and regional seismic stations (e.g., Italy, Greece, Cyprus, Turkey) surrounding the epicenter. The regional seismic data is available online and is here used to improve the azimuthal coverage. The hypocenteral parameters are determined using data set of 48 seismograms and based on running two technical programs; the HYPOINVERSE program included in ATLAS software, Version 2.11, provided by Nanometrics Inc. and the standard linearized inversion program, HYPOCENTER 3.2 (Lienert et al. 1986; Lienert and Havskov 1995) that is operated under SEISAN software. The earth model of seismic velocities is here used after (Makris et al. 1979).

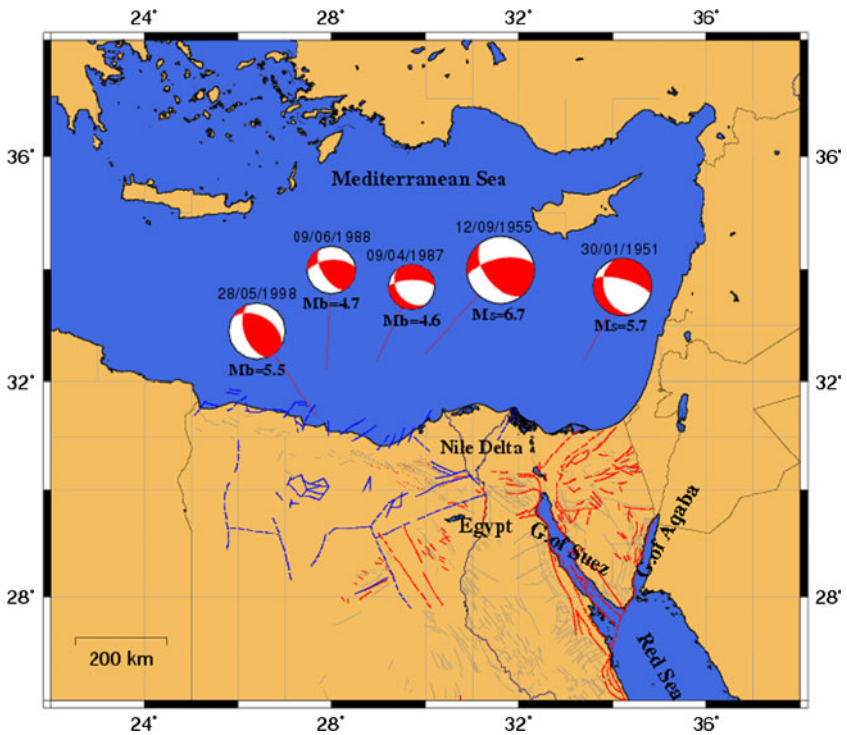

Fig. 3 Focal mechanisms of the significant earthquakes that took place in the Egyptian continental margin

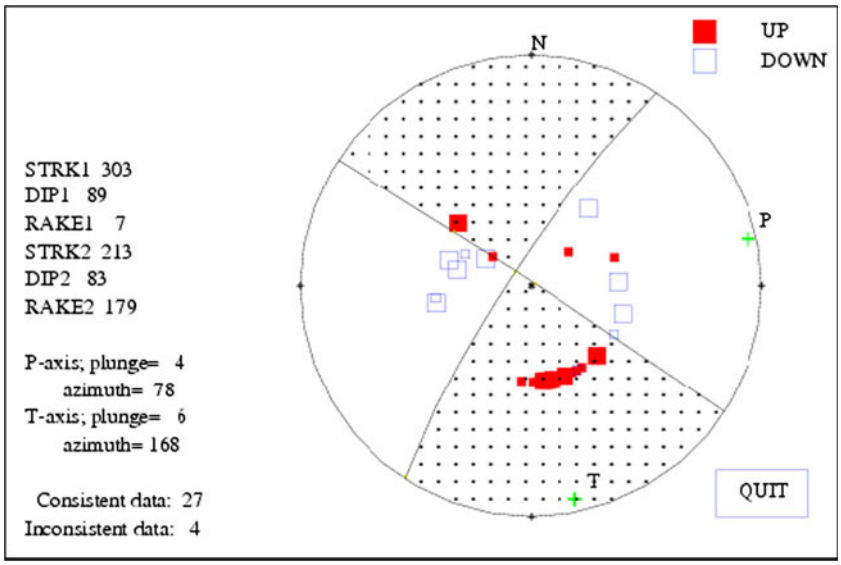

Fig. 4 Fault plane solution of the 19 October 2012 earthquake based on the first motion polarities of P-waves

The fault plane solution of the 19 October 2012 earthquake has been carried out based on the direction of the first motion of P-waves of 31 seismograms distributed around the epicenter with gab azimuth = 42.5°. The analysis is performed using the software package of Suetsugu (1998). In the current work, the low-quality data is excluded from our analysis due to low signal-to-noise ratios, unclear identification of the first onset, and inaccurate onset times. The obtained solution shows a left lateral strike-slip faulting mechanism trending NW–SE (Fig. 4). Table 1 summarizes the nodal planes' parameters. These results are in a good agreement with the solution given by the INGV (Instituto Nazionale Di Geofisica e Vulcanologia) which reflects a left lateral strike-slip fault trending NW–SE with gab azimuth = 55° (http://autorcmt.bo.ingv.it/QRCMT-on-line/QRCMT12-on-line/E1210190335A.html).

The focal mechanism is also carried out using FOCMEC program (Snoke et al. 1984) under SEISAN, which uses the direction of the first P-waves onset and the amplitude ratios of P-wave, horizontal S-wave (SH), and vertical S-wave (SV). This technique depends upon the P-waves and amplitude inversion method (Ebel and Bonjer 1990). FOCMEC program performs an efficient systematic search of the focal sphere and reports acceptable solutions based on selection criteria for the number of polarity uncertainties. The selection criteria for both polarities and angles allow correction or weightings for near-nodal solutions (Fig. 5), which demonstrates that the compression and dilatation areas are in a good distribution due to the good coverage by seismic stations. The final focal mechanism obtained by FOCMEC program shows a reverse fault with strike-slip component trending NW–SE to NE–SW (Fig. 6). Its parameters are listed in Table 2. This solution agrees with the solutions of the United States Geological Survey (USGS) and the International Seismological Centre (ISC) online bulletins.

Source parameters

The source parameters provide important information in seismic hazard assessment of any region. In order to obtain further information about the physical properties of the earthquake source, it is necessary to find out a complete set of the source parameters such as the focal location, magnitude, seismic moment, source dimension, stress drop, and average seismic slip. Several studies (Hanks and Wyss 1972; Thatcher and Hanks 1973; Tucker and Brune 1977; Singh et al. 1979; Fletcher 1980; Sharma and Wason 1994; Bansal 1998, Thakur and Kumar 2002; Kumar 2011) have made notable contribution in the source

Table 1 Parameters of fault plane solution of the 19 October 2012 earthquake based on the first motion polarities of P-waves

Date	Origin time (GMT)	Location		P-axis		T-axis		Nodal plane 1			Nodal plane 2			Depth (km)	M_L
		Lat	Long	Az	Pl	Az	Pl	S	D	R	S	D	R		
19102012	03:35:14	32.35°	31.27°	78	04	168	06	303	89	7	213	83	179	12.7	5.1

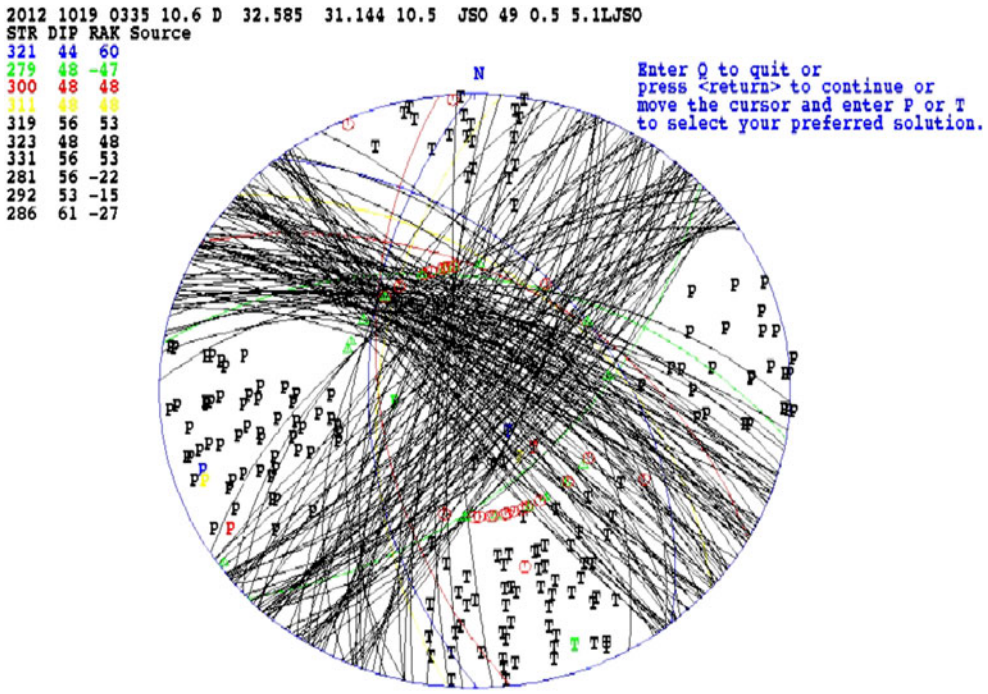

Fig. 5 Multi-solutions plot for the 19 October 2012 earthquake obtained by FOCMEC program

parameters investigations following the Brune's theory (Brune 1970, 1971), which describes the far-field displacement amplitude spectra as the physical process that release energy at source. Uncertainties in source parameter determinations are directly related to theoretical and observational uncertainties in the specification and determination of far-field displacement spectra. Once the corrected displacement amplitude spectrum is determined, the frequency spectral level (Ω_0),

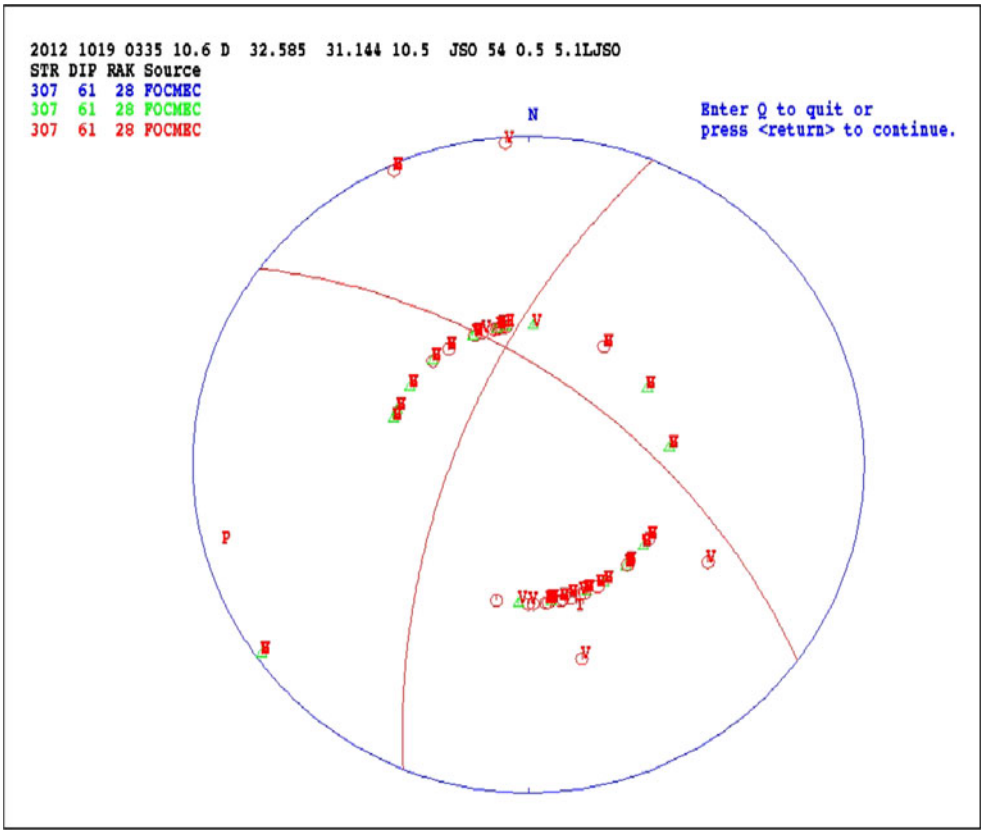

Fig. 6 Final focal mechanism of the 19 October 2012 earthquake obtained by FOCMEC program and based on the P-wave polarities and amplitude ratio of P-, SH-, and SV-waves

Table 2 Parameters of fault plane solution of the 19 October 2012 earthquake obtained by FOCMEC program and based on the P-wave polarities and amplitude ratio of P-, SH-, and SV-waves

Date	Time (GMT)	Location		Nodal plane			Depth (km)	M_L	Mw
		Lat	Long	S	D	R			
19102012	03:35:10	32.58°	31.14°	307	61	28	10.5	5.1	4.9

corner frequency (f_c), t^* (the average attenuation path), and γ were varied to converge the best fits to the Fourier spectrum using least squares nonlinear technique. By assuming Brune's model ($\gamma = 2$), the number of free parameters decreases from four to three and the fit is more robust (Hough 1996).

This study presents an attempt to calculate the source parameters of the 19 October 2012 earthquake. Firstly, the original seismograms of some selected stations are retrieved for removing the effects of free surface, instrument response, and geometrical spreading. Secondly, the vertical components are selected to skip corrections of the site effect. The low-frequency spectral level (Ω_0) and corner frequency (f_c) are estimated from the displacement amplitude spectra of these seismograms (Fig. 7). The seismogram analysis provides an

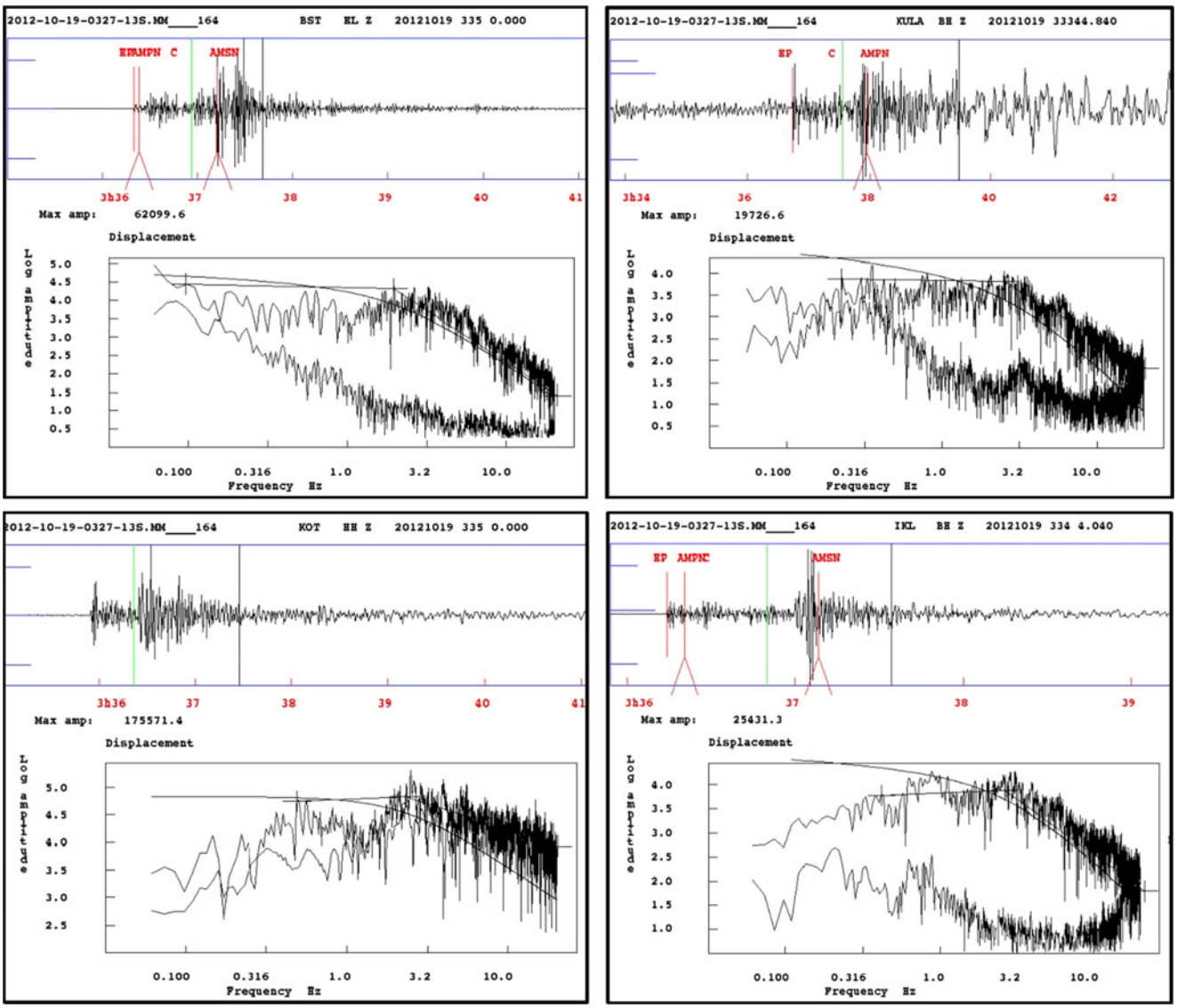

Fig. 7 Vertical component seismograms of the stations BST and KOT in Egypt and KULA and IKL in Turkey of the 19 October 2012 earthquake (*upper*); the displacement amplitude spectra (*lower*), presented by the signal spectrum (*top*), noise spectrum (*bottom*), observed spectral (*smooth curve*), low-frequency, and high-frequency asymptotes with their intersection point as a corner frequency (*straight lines*), respectively

Table 3 Source parameters of the 19 October 2012 earthquake

f_c (Hz)	$\Delta\sigma$ (MPa)	r (km)	M_0 (Nm)	Mw
1.473	22.1	0.7	2.80E + 16	4.9

accurate seismic moment (M_0). In frequency domain, the amplitude spectra have low-frequency asymptote levels, Ω_0, which related directly to seismic moment (Brune 1970) as follows:

$$Mo = 4\pi\rho v^3 R\Omega_0/R(\Theta\Phi) \quad (1)$$

where ρ and ν are the density and the wave velocity at the source, R is the hypocentral distance, Ω_0 is the low-frequency spectral amplitude, and $R(\Theta\Phi)$ is the radiation pattern coefficient. In this work, the shear-wave velocity near the source zone is taken as 3.5 km/s and average density of the medium (ρ) is taken as 2.67 g/cm^3, and the average radiation pattern is 0.63, $S\alpha$ is free surface amplification = 2.

The source dimension could be described by different factors such as the area of the fault (A), the length of the rectangular fault (L), and the radius of the equivalent circular fault (r), where $L \approx 2r$. It controls the period of seismic waves, determines the deformed area, and can consequently be used in the calculation of other source parameters (e.g., stress drop and average slip). The fault length is inversely proportional to the corner frequency and can be calculated from the wave spectra as follows:

$$r = 0.37\nu/f_c \quad (2)$$

where ν is the wave velocity and f_c is the corner frequency of the wave spectrum.

The stress drop ($\Delta\sigma$) describes the difference in shear stress on the fault plane before and after the slip. When a complete stress released is assumed, the stress drop for a circular fault can be calculated from the relation between the seismic moment and the fault radius using the formula of Brune's (1970) as follows:

$$\Delta\sigma = 0.44\, M_0/r^3 \quad (3)$$

where M_0 is the seismic moment and r is the fault radius.

The moment magnitude M_w is an important parameter in earthquake hazard assessments. The time window used for spectral determination of M_w must be at least as long as the rupture time to include all the energy. Thus, P-spectra of large earthquakes at short distances might not be possible. The moment magnitude developed by Kanamori (1977) and Hanks

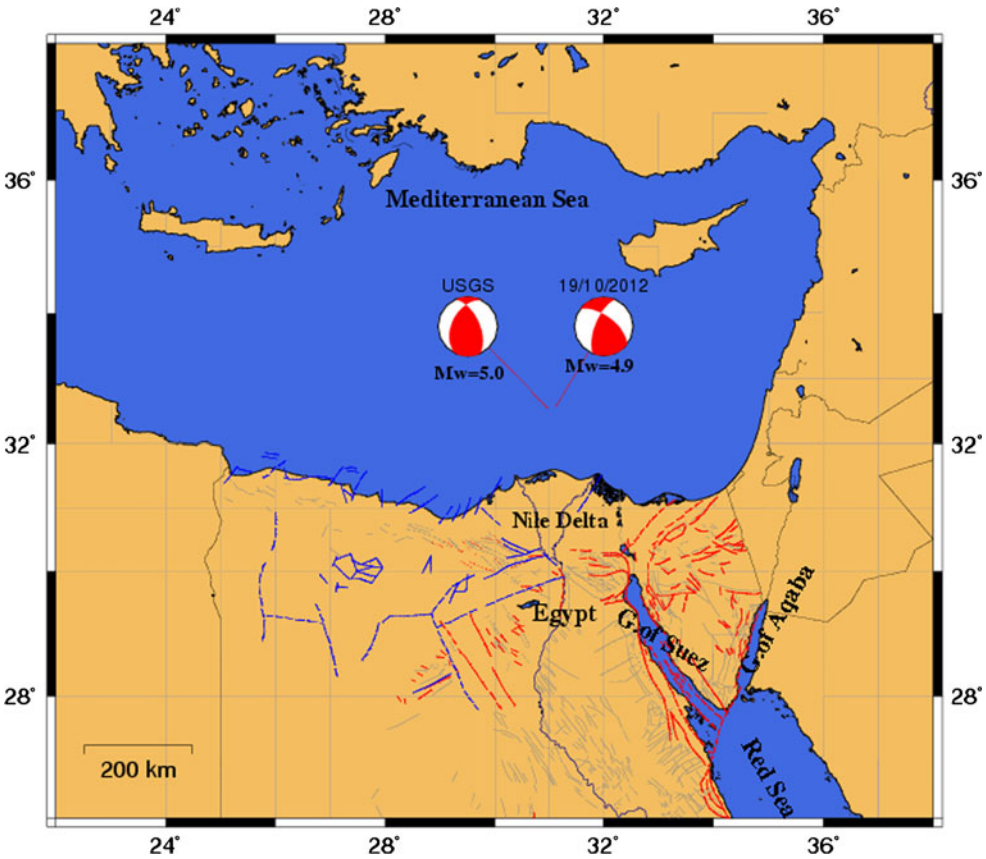

Fig. 8 Fault plane solution of the 19 October 2012 earthquake obtained from this study and from USGS bulletin

and Kanamori (1979) is defined according to the following IASPEI-recommended standard form:

$$Mw = 2/3*\log10\ (M_0) - 6.07 \quad (4)$$

where M_0 is the seismic moment, M_w = 2/3 * log10 (M_0) − 10.73 if moment is in dyne * cm (Kanamori 1977).

Table 3 summarizes the calculated source parameters for the 19 October 2012 northern Egyptian continental margin earthquake.

Discussion and conclusion

The northern Egyptian continental margin is located to the south of the Mediterranean Sea Ridge where the sea floor is occupied by the Nile Deep Sea Fan, Eratosthenes Seamount, and Herodotus basin. It represents the northeastern portion of the North African passive continental margin. Economically, this region is of great importance as a hydrocarbon productive zone. Previous studies demonstrate that this region is characterized by a complex tectonic setting accompanied by seismic activity. The moderate size earthquake (M_L = 5.1) of 19 October 2012 occurred in this region, which has experienced the 12 September 1955 earthquake (Ms = 6.7).

We introduced a detailed fault plane solution for the 19 October 2012 earthquake by using the waveform data recorded by the Egyptian National Seismological Network (ENSN). In order to improve the azimuthal coverage, recordings from regional seismographs were included in our analysis. The analysis was performed using the first motion polarities of P-wave and the amplitude ratios of P-, SH-, and SV-waves. The obtained fault plane solution based on the first P-wave onset of 31 seismograms around the epicenter showed a left lateral strike-slip faulting mechanism, agreeing with the solution given by the INGV. Analysis based on the P-wave polarities and amplitude ratios of P-, SH-, and SV-waves revealed a reverse fault with strike-slip component trending NW–SE to NE–SW in conformity with the N–S compression along the Hellenic Arc convergence zone. This mechanism corresponds to the solution of the USGS online bulletin (Fig. 8). We prefer this solution since it shows a good agreement with the compressional stress field which is affecting the source region due to the relative movement between African and Eurasian plates. Moreover, it is compatible with the fault plane solutions of most of the past earthquakes in the area which shown in Fig. 3.

At the second part of this study, we calculated the source parameters, which provide quantitative information about the physical properties of the earthquake source. Using the Brune's model, the source dynamic parameters of the 19 October 2012 earthquake are estimated as corner frequency = 1.47 Hz, fault radius = 0.7 km, stress drop = 22.1 MPa, seismic moment = 2.80E + 16 Nm, and moment magnitude (M_w = 4.9), similar to that estimated by the USGS (Mwc = 5.0).

Acknowledgments The analysis described here, was performed using data from the Egyptian National Seismological Network (ENSN), USGS, and ORFEUS. We thank all these organizations for providing the valuable data. We wish to thank the anonymous reviewers for their constructive comments.

References

Abdel Aal A, Lelek JJ (1994) Structural development of the northern Sinai, Egypt, and its implication on hydrocarbon prospectively of the Mesozoic. In: Al Husseini, M.I. (Ed.), Selected Middle Conference, Geo. 94. Gulf Petrolink, Bahrain, Geoarabia 1:15–30

Abou Elenin K, Hussein H (2007) Source mechanism and source parameters of May 28, 1998 earthquake, Egypt. JSEE 11(3):259–274

Abu Elenean K (1993) M.Sc. thesis. In: Seismotectonics of the Mediterranean region, north of Egypt and Libya. Mansoura University, Mansoura, Egypt

Abu Elenean KM (1997) Ph.D. thesis, Fac. Sci. In: A study on the seismotectonic of Egypt in relation to the Mediterranean and Red Sea tectonics. Ain Shams Univ., Cairo, Egypt

Abu El-Nader IF, El Gabry MN, Hussein H, Hassan HM, Elshrkawy A (2013) Source characteristics of the Egyptian Continental margin earthquake, 19 October 2012. Seis Res Lett, V 84(6):1062–1065. doi:10.1785/0220120172

Ambraseys N, Melville C, Adams R (1994) The seismicity of Egypt, Arabia and the Red Sea: a historical review. Cambridge University Press

Badawy A (1996) PhD thesis. In: Seismicity and kinematic evolution of the Sinai plate. L. Eötvös Univ., Budapest, p. 115

Badawy A (1999) Historical seismicity of Egypt. Acta Geod Geophys Hung 34(1–2):119–135

Badawy A, Horváth F (1999a) Recent stress field of the Sinai subplate region. Tectonophysics 304:385–403

Badawy A, Horváth F (1999b) Seismicity of the Sinai subplate region: kinematic implications. J. Geodynam. 27:451–468

Badawy A, Mohamed G, Omar K, Farid W (2015) The northern Egyptian continental margin. J Afr Earth Sci 101:177–185. doi:10.1016/j.jafrearsci.2014.09.009

Bansal BK (1998) Determination of source parameters for small earthquake in the Koyna region. 11th Symposium on Earthquake Engineering. Roorkee 1:57–66.20

Brune J (1970) Tectonic stress and the spectra of seismic shear waves from earthquakes. J Geophys Res 75:4997–5009

Brune J (1971) Correction. J Geophys Res 76:5002

Camera L, Sage F, Klaeschen D, Ribodetti A, Mascle J (2004) New constraints on the structure of the Eastern Nile continental margin from MCS data pre-stack depth migration. European Geosciences Union, Nice, France Abstract.

Costantinescu L, Rubrechtova L, Enescu D (1966) Mediterranean Alpine earthquake mechanisms and their seismotectonic implications. Geophys. J. R. Astronom. Soc. 10:347–368

Dolson JC, Shann MV, Matbouly SI, Hammouda H, Rashed MR (2000) Egypt in the twenty-first century: petroleum potential in offshore trends. Geoarabia 6:211–230

Ebel JE, Bonjer KP (1990) Moment tensor inveriosn of small earthquakes in southwestern Germany for fault plane solution. Geophys J Int 101:133–146

EL-Banna MM, Frihy OE (2009) Natural and anthropogenic influences in the northeastern coast of the Nile Delta Egypt. Environ Geol 57(7):1593–1602

Fletcher JB (1980) Spectra from high dynamic range digital recordings of Oroville, California aftershocks and their source parameters. Bull Seis Soc Am 70:735–755 14

Garfunkel Z (1998) Constraints on the origin and history of the Eastern Mediterranean Basin. Tectonophysics 298:5–35

Garfunkel Z (2004) Origin of the Eastern Mediterranean Basin: a reevaluation. Tectonophysics 391:11–34

Guiraud R, Bosworth W (1999) Phanerozoic geodynamic evolution of Northeastern Africa and the northwestern Arabian platform. Tectonophysics 315:73–108

Hanks TC, Kanamori H (1979) A moment magnitude scale. D Geophys Res 84:2348–2350

Hanks TC, Wyss M (1972) The use of body-wave spectra in the determination of seismic-source parameters. Bull Seismol Soc Am 62(1972):561–589

Hough SE (1996) Observational constraints on earthquake source scaling: understanding the limits in resolution. Tectonophysics 261:83–95

Hussein, H. M., Korrat, I. M., El Sayed, A. (2001) Seismicity in the vicinity of Alexandria and its implication to seismic hazard. In: Proc. Of the Second International Symposium on Geophysics, Tanta, 2, pp. 57–64

Kanamori H (1977) The energy release in great earthquakes. D Geophys Res 82:2981–2987

Korrat IM, El Agami NL, Hussein HM, El Gabry MN (2005) Seismotectonics of the passive continental margin of Egypt. J Afr Earth Sci 41:145–150. doi:10.1016/j.jafrearsci.2005.02.003

Kumar A (2011) Study of earthquake source parameters using micro earthquakes and strong motion data, Thesis submitted to Indian Institute of Technology. Roorkee 21

Le Pichon X, Augustithis SS, Mascle J (1982) Geodynamics of the Hellenic Arc and Trench. Tectonophysics 86:1–304

Lienert BRE, Havskov J (1995) A computer program for locating earthquakes both locally and globally. Seism Res Lett 66:26–36

Lienert BRE, Berg E, Frazer LN (1986) Hypocenter: an earthquake location method using centered, scaled, and adaptively least squares. Bull Seismol Soc Am 76:771–783

Loncke, L. (2002) Le delta profond du Nil: structure et evolution depuis le Messinien, The'se de doctorat de l'Universite'P. et M. Curie (Paris 6).

Maamoun M, Megahed A, Allam A (1984) Seismicity of Egypt. Bull HIAG 4:109–160

Makris J (1976) A dynamic model of the Hellenic Arc deduced from geophysical data. Tectonophysics 36:339–346

Makris, J., Stofen, B., Vees, R., Allam, A., Maamoun, M., Shehata, W. (1979) Deep seismic sounding in Egypt. Part I: the Mediterranean Sea between Crete-Sidi Barani and the coastal area of Egypt

Mascle J, Benkhelil J, Bellaiche G, Zitter T, Woodside J, Loncke L (2000) Marine geologic evidence for a Levantine-Sinai plate, a missing piece of the Mediterranean puzzle. Geology 28(9):779–782

Mascle J, Sardou O, Loncke L, Migeon S, Camera L, Gaullier V (2006) Morphostructure of the Egyptian continental margin: insights from Swath Bathymetry Surveys. Mar Geophys Res 27:49–59. doi:10.1007/s11001-005-1559-x

McKenzie DP (1970) Plate tectonics of the Mediterranean region. Nature 226:239–243

McKenzie DP (1972) Active tectonics of the Mediterranean region. Geophys J R Astron Soc 30:109–185

Morelli C (1978) Eastern Mediterranean geophysical results and implications. Tectonophysics 46(3–4):333–346

Robertson AHF (1998) Tectonic significance of the Eratosthenes Seamount: a continental fragment in the process of collision with a subduction zone in the eastern Mediterranean (ocean drilling program leg 160). Tectonophysics 29:863–882

Ross R, Uchupi I (1977) The structure and sedimentary history of the SE Mediterranean Sea. Bulletin American Associations Petroume Geology 61:879–902

Sharma ML, Wason HR (1994) Occurrence of low stress drop earthquakes in the Garhwal Himalaya region. Phys Earth Planet Inter 85:265–272. 19

Singh DD, Rastogi BK, Gupta HK (1979) Spectral analysis of body waves for earthquakes and their source parameters in the Himalaya and nearby regions. Phs Earth Planet, Inter 18:143–15213

Snoke JA, Munsey JW, Teague AG, Bollinger GA (1984) A programme for focal mechanism determination by combined use of polarity and SV-P amplitude ratio data. Earthquake Note:55–15 pp.

Sofratom Group (1984) Regional geology, tectonics and seismology, pp. 21–32 (Chapter 3).

Suetsugu D (1998) Practice on source mechanism, International Institute of Seismology and Earthquake Engineering (IISEE) lecture note, Tsukuba, p. 104 pp

Thakur VC, Kumar S (2002) Seismotectonics of the Chamoli earthquake of March 29, 1999 and earthquake hazard assessment of Garhwal–Kumaon region, NW Himalaya. Himal Geol 23(1–2):113

Thatcher W, Hanks TC (1973) Source parameters of Southern California earthquakes. J Geophys Res 78:8547–8576 10

Tucker BE, Brune JN (1977) Source mechanism and m-M analysis of aftershocks of the San Fernando earthquake. J Geophys 49:371–426 12